Science World Journal Vol. 17(No 1) 2022
www.scienceworldjournal.org
ISSN: 1597-6343 (Online), ISSN: 2756-391X (Print)
Published by Faculty of Science, Kaduna State University

GROUNDWATER EXPLORATION USING 2D RESISTIVITY IMAGING WITHIN ABUJA MUNICIPAL AREA COUNCIL, NIGERIA

*Ezeamaka Grace Ozioma, Mallam Abu, Osagie Abel Uyimwen

Department of Physics, University of Abuja, Nigeria

*Corresponding Author Email Address: ezeamakagrace047@gmail.com

ABSTRACT

The fast-growing population of Abuja, Nigeria has over-stretched the public water supply capacity of the city. Like in many expensive cities, people live mostly in a conurbation of towns within Abuja metropolitan area (like the Kurudu area) where the public water supply is inadequate. The inhabitants are compelled to explore other sources of water such as stream water, shallow well water e.t.c for survival. Groundwater is a readily available source and its exploration becomes a necessity. In this research, a two-dimensional (2D) electrical resistivity imaging survey technique is carried out within the Kurudu area of the Abuja Municipal Area Council in Nigeria. The ABEM Terrameter (SAS 1000) with Schlumberger configuration is used to acquire resistivity data from eleven profiles (9 profiles laid vertically, each with a lenght of 122 m and two profiles laid horizontally of lenght 82 m and 40 m). The RES2DINV is used to interpret the data and to model the subsurface. Three geoelectric layers with varying resistivities are identified beneath the study area. The top layer which have been inferred to as the lateritic clay/sandy clay has resistivity range of 5 - 3500 Ohm meters (Ωm) with thickness of 1.5 - 2.55 meters (m). The second layer comprises of the weathered/fractured basement with depths of 1.5 - 15.8 m and ranges in resistivity values between 1 Ωm and 3000 Ωm. The bedrock which makes the third layer at depths of 10 - 15.8 m has resistivity range of 1000 Ωm to 3500 Ωm. The result of the inverse resistivity model suggests the presence of an eleven-meter aquifer thickness in the western flank of the study area. The average depth of the subsurface is about 15 meters.

Keywords: Groundwater, resistivity, modelling

INTRODUCTION

The increased interest in recent years in underground sources of water has led to a need for more intensive studies of the geometry and properties of aquifers. Geophysics has played a useful part in such investigations. Clean water availability and accessibility is a challenge in many parts of the world. In many parts of Africa, useful long-term data about water resources are unavailable (Seiler, 2000). Over the years, different methods have been developed to understand groundwater movement and the different processes that occur in reservoirs (which may be natural or influenced by human activities). Understanding the chemical reactions, fluxes, ages and mixing processes occurring in reservoirs is the basis on which strategies are developed for exploration, exploitation and protection of groundwater (Seiler, 2000).

The developmental programmes since the oil boom era in Nigeria and the growing population in the last four decades have put tremendous pressure on the nation's available resources (Adelana and Olasehinde, 2003). In the same vein, water supply projections to the Federal Capital Territory (FCT), Abuja, Nigeria, has become inadequate. The Lower Usman Dam Water Works has a production capacity of 8000 cubic meters per hour. The water supply capacity of the dam has remained the same in 25 years for a population of 500,000 residents of Abuja (CIWAT, 2010; FCT MGDs, 2010). Over the years, there has been an unprecedented influx of people to the FCT for economic reasons and for safety from the crisis-ridden towns in the country (AIIC, 2009; FCT MDGs, 2010). In 2009, Abuja is reported to be fastest growing city in Africa (AIIC, 2009) with an unprecedented annual growth rate of 13%. Public water supply is therefore, inadequate to meet the demand for water in Abuja. The inhabitants of the city are compelled to explore other sources of water for survival. Groundwater is the readily available source. The need, therefore, arises to explore for groundwater resources to supplement the limited surface water to meet the needs of the populace.

Electrical resistivity imaging is used widely for environmental surveys and it is one of the geophysical surveys used for groundwater exploration. This technique has been used to determine the subsurface resistivity anomalies and has become popular for investigating water movement in the Vadoze Zone (Griffiths & Barker, 1993; Hamzah et al., 2006; Samsudin et al., 2000, 2001). The aim of the present study is to explore for groundwater potential within the Kurudu area of the Abuja Municipal Area Council, Nigeria. In order to achieve this aim, the study carried out electrical resistivity survey within the area, and used two-dimensional (2D) electrical resistivity imaging technique to determine the aquifer thickness and depth within the study area, to estimate the geological strata and to infer their electrical properties.

MATERIALS AND METHODS

The Study Area

The study area is approximately 14,000 m^2 (Fig. 1) located in Kurudu— a sub-urban town of the Abuja Municipal Area Council (AMAC). Its coordinates are lattitude $8^0 55' 53''$North and longitude $7^0 33' 0''$East. Kurudu is a major town around the Asokoro Area— a conurbation of towns within Abuja metropolitan area. Kurudu's neighbouring towns are new Nyanya, new Karu, Guzape and AYA. Kurudu village is a result of rapid growth and expansion of administrative and economic activities of Abuja into neighbouring towns, coupled with the evacuation of many people from Abuja cities by the FCT administration.

Science World Journal Vol. 17(No 1) 2022
www.scienceworldjournal.org
ISSN: 1597-6343 (Online), ISSN: 2756-391X (Print)
Published by Faculty of Science, Kaduna State University

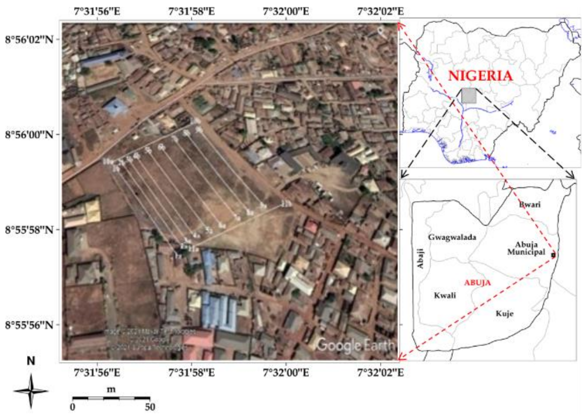

Figure 1: Location of the study area showing profile layouts (white lines)

Materials

The electrical resistivity data are collected with the use of a computer-controlled measurement systems which is the ABEM LUND Resistivity Imaging System (Fig. 2). The data acquisition process is completely controlled by computer software called Resist, which checks that all the electrodes are connected and properly grounded before measurement starts. After adequate grounding is achieved the software scans through the measurement protocol selected. The system consists of a basic unit, a standard resistivity meter (ABEM Terrameter SAS1000), a (4 × 64) multi-channel relay matrix switch unit called Electrode Selector ES 464, four multi-conductor electrode cables wound on reels each with 21 take-outs, stainless steel electrodes, cable jumpers, and various connectors. The system is compatible with a portable PC-type computer or notebook (laptop). The Signal Averaging System (SAS) functionality of the equipment allows for an average value to be obtained from the result of consecutive measurements. Signal Averaging System (SAS) results are more reliable than those obtained from single- short systems. The SAS 1000 can operate in different modes, e.g., resistivity, and self-potential and induced polarization. In all its modes it is capable of measuring simultaneously in four channels thus making it suitable in all sorts of resistivity surveys.

Figure 2: The ABEM LUND imaging system and the Terrameter SAS1000

Methods

The fieldwork was carried out between April and July 2019. Nine profiles, 5 m (meters) spacing, each of which is 122 m long with NW-SE orientation are considered in this work (Fig. 1). In addition, two profiles that are 82 m and 40 m each, and with NE-SW orientation are taken across the beginnings and ends of the nine profiles (Fig. 1). The Schlumberger electrode array is used to acquire resistivity data from the eleven profiles. The Schlumberger array provides for a high signal-to-noise ratio, has excellent vertical resolution and good depth sensitivity. The effect of near-surface, lateral in-homogeneities affect Schlumberger measurements less than it affects the Werner measurements and the interpretation techniques are more fully developed (Maliva 2016). The orientation of the profiles was in the NW-SE direction with a NE-SW azimuth. This was employed to ensure a desirable field space for the work. This study used the Electrical Resistivity Tomography (ERT) method to generate 2D images of the subsurface resistivity distribution. With this method, features with electrical properties differing from those of the surrounding material may be located and characterized in terms of electrical resistivity, geometry, and depth of burial.

For the set-up, which was used on the field, a total of 41 electrodes are recognized because of the overlap of the 21st electrode of cable 1 with the 1st electrode of cable 2 at the layout center, which is recognized as a single electrode. An electrode test is carried out immediately to check for electrodes with bad ground contact. The connectors are also checked for unsatisfied electrode positions. Electrodes are tested pair-wise against each other starting from the outermost electrodes going toward the center. The electrode test checked for possible transmission of current through all the electrodes. The test took a couple of minutes but saves time afterward; because the program may stop depending on poor electrode contact. The measurement may also stop if the batteries for either the Terrameter or the Electrode Selector are low. The program continues to measure automatically using the two electrode cables when the contact is satisfactory. After measurements have been taken along a profile, the terrameter is switched off and taken to the next profile, with the same sequence repeated. To obtain a good 2D picture of the subsurface, the coverage of the measurements must be 2D as well.

The RES2DINV software, a computer program that automatically determines a two- dimensional (2D) resistivity model for the subsurface for the data obtained from the electrical resistivity survey, was used to process the raw resistivity data that was downloaded from the terrameter. The forward problem is solved through a finite difference algorithm, whose main features are a versatile user-defined discretization of the domain and a new approach to the solution of the inverse Fourier transform. The forward modeling subroutine is used to calculate the apparent resistivity values. The inverse procedure is based on an iterative smoothness-constrained least-squares algorithm. This computer program uses smoothness constrained non-linear least- squares optimization inversion technique to convert measured apparent resistivity values to true resistivity values and plot them in cross-sections. The inversion process removes geometrical effects from the pseudo-section and produces an image of true depth and true formation resistivity. One advantage of this method is that the damping factor and flatness filter can be adjusted to suit different types of data. The program creates a resistivity cross-section, calculates the apparent resistivities for that cross-section, and compares the calculated apparent resistivities to the measured apparent resistivities. The iteration continues until a combined smoothness constrained objective function is minimized. Interpretation of resistivity data consists of two steps: a physical interpretation of the measured data, resulting in a physical model (geo-electric model), and a geological interpretation of the resulting physical parameters (Dahlin, 2001). The large-scale data were processed with the state-of-the-art interpretation technique, called the 2D smoothed damped least-squares inversion algorithm. The true geo-electric models/pseudo-sections of the profiles were formed using automatic 2D smoothness constrained least-squares inversion because the smoothness constrain prevents unstable and extreme solutions, whereas a quasi-Newton reduces the numerical calculations (Loke and Barker, 1996). Quite often a useful amount of information can be extracted from a pseudo-section by a careful inspection of the contour pattern and apparent resistivity values, particularly, if some geological controls are available.

RESULTS AND DISCUSSION

The results of 2D inversion are shown in figures 3-13. For profile 1 (Fig. 3), the upper part of the layer reveals resistive materials at the top layer. The resistivity values range from 150-500 Ωm (Ohm meters) with a thickness of about 2.55 m. The top layer (lateritic clay/sandy clay) is underlain by a weathered basement, which has a depth range of 2-13.5 m with resistivity values between 10 Ωm to 150 Ωm. The high resistivity values (200 Ωm – 800 Ωm) is seen at the depth range of 12.5 m to 15.8 m at the southern part of the section. Profile 2 shows resistive materials within the top layer (Fig. 4). The resistivity values range from 100-1900 Ωm with a thickness of about 2.55 m. The second layer which is at a depth range of 2-15.8 m has resistivity values ranging between 15-1900 Ωm. Areas with low resistivity values are observed between lateral distance 2-16 m at a depth range of 1-7 m where the resistivity values of the material ranges between 15-20 Ωm, lateral distance 50-62 m at a depth range of 5-12 m where the resistivity values of the material is about 15 Ωm and at lateral distance 102-112 m at a depth range of 5-12 m, where the resistivity values of the material is about 15 Ωm.

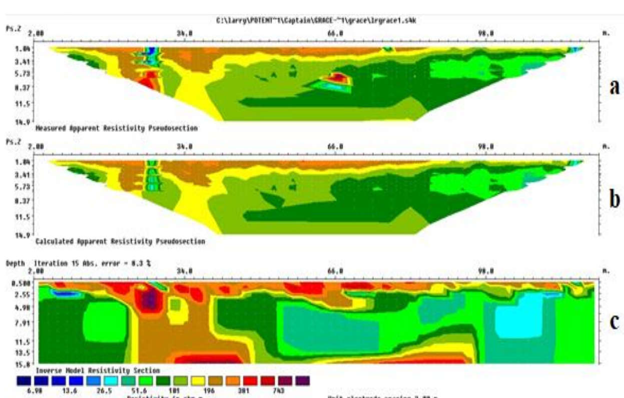

Figure 3: 2D inversion result of profile 1: (a) measured apparent resistivity pseudo-section; (b) calculated apparent resistivity pseudo-section; and (c) inverse model resistivity section.

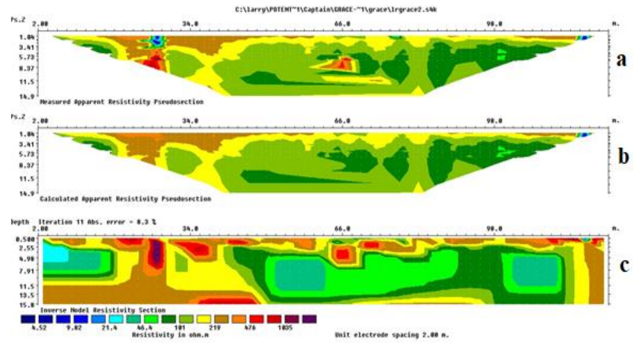

Figure 4: 2D inversion result of profile 2. (a) measured apparent resistivity pseudo-section, (b) calculated apparent resistivity pseudo-section, and (c) inverse model resistivity section.

Profile 3 (Fig. 5) also reveals resistive materials at the top layer. The resistivity values range from 80-1300 Ωm with a thickness of about 2 m. The top layer (lateritic clay/sandy clay) is underlain by a weathered basement, which has resistivity values between 10-100 Ωm, with a depth range of 2-15.8 m. This was absent between lateral distance of 30-40 m where the resistivity of the materials ranges between 200-300 Ωm. The upper part of the layer reveals resistive materials at the top layer in profile 4 (Fig. 6). The resistivity values range from 200-800 Ωm with a thickness of about 2.5 m. The second layer has a depth range of 2.5-15. 8 m with resistivity values between 30-800 Ωm. This layer is interpreted as the fractured basement.

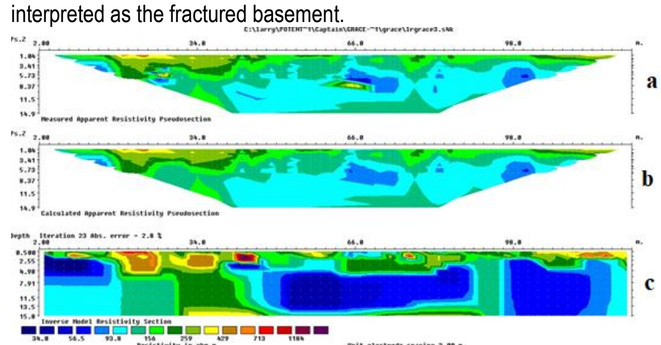

Figure 5: 2D inversion result of profile 3. (a) measured apparent resistivity pseudo-section, (b) calculated apparent resistivity pseudo-section, and (c) inverse model resistivity section.

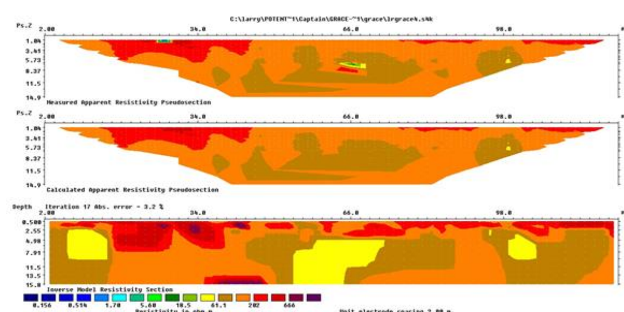

Figure 6: 2D inversion result of profile 4. (a) measured apparent resistivity pseudo-section, (b) calculated apparent resistivity pseudo-section, and (c) inverse model resistivity section.

Science World Journal Vol. 17(No 1) 2022
www.scienceworldjournal.org
ISSN: 1597-6343 (Online), ISSN: 2756-391X (Print)
Published by Faculty of Science, Kaduna State University

The upper part of the layer reveals resistive materials at the top layer in profile 5 (Fig. 7). The resistivity values range from 60-3400 Ωm (Ohm meters) with a thickness of about 2 m. The top layer (lateritic clay/sandy clay) is underlain by a weathered basement, which has a depth range of 2-15.8 m with resistivity values between 10-3000 Ωm. The upper part of the layer reveals resistive materials at the top layer in profile 6 (Fig. 8). The resistivity values range from 50-3500 Ωm (Ohm meters) with a thickness of about 2 m. The top layer (lateritic clay/sandy clay) is underlain by a weathered basement, which has a depth range of 2-15.8 m with resistivity values between 10-1300 Ωm.

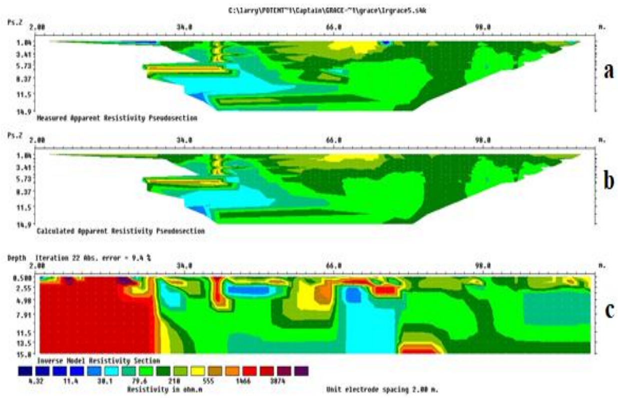

Figure 7: 2D inversion result of profile 5. (a) measured apparent resistivity pseudo-section, (b) calculated apparent resistivity pseudo-section, and (c) inverse model resistivity section.

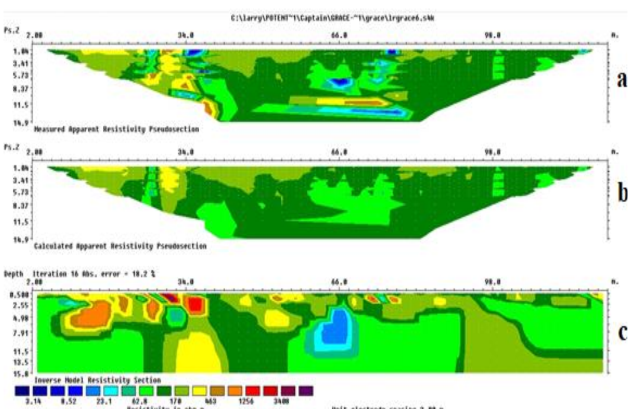

Figure 8: 2D inversion result of profile 6. (a) measured apparent resistivity pseudo-section, (b) calculated apparent resistivity pseudo-section, and (c) inverse model resistivity section.

The upper part of the layer reveals resistive materials at the top layer in profile 7 (Fig. 9). The resistivity values range from 80-1300 Ωm (Ohm meters) with a thickness of about 2.5 m. The top layer (lateritic clay/sandy clay) is underlain by a weathered basement, which has a depth range of 2.5-13.5 m with resistivity values between 10-220 Ωm. The high resistivity values (220-1200 Ωm) are seen at the center of the section showed that the subsurface materials are resistive. The upper part of the layer reveals resistive materials at the top layer in profile 8 (Fig. 10). The resistivity values range from 100-900 Ωm (Ohm meters) with a thickness of about 1.5 m. The high resistivity extends to a depth of 15.8 m. The top layer is underlain by a layer, which has a depth range of 1.5-15.8 m with resistivity values between 15-900 Ωm.

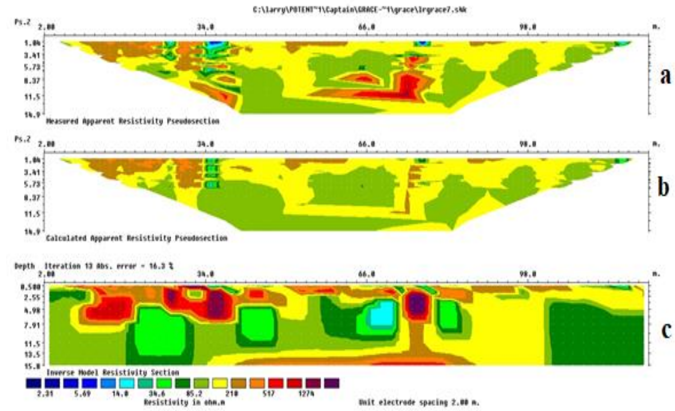

Figure 9: 2D inversion result of profile 7. (a) measured apparent resistivity pseudo-section, (b) calculated apparent resistivity pseudo-section, and (c) inverse model resistivity section.

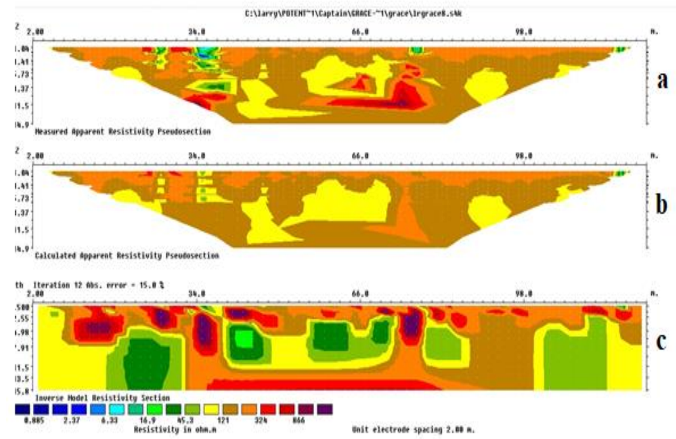

Figure 10: 2D inversion result of profile 8. (a) measured apparent resistivity pseudo-section, (b) calculated apparent resistivity pseudo-section, and (c) inverse model resistivity section.

The upper part of the layer reveals resistive materials at the top layer in profile 9 (Fig. 11). The resistivity values range from 50-800 Ωm (Ohm meters) with a thickness of about 2 m. The top layer (lateritic clay/sandy clay) is underlain by a weathered basement, which has a depth range of 2-8 m with resistivity values between 10-150 Ωm. The third layer is characterized by resistive materials with resistivity values ranging between 50-400 Ωm at a depth range of 8-15.8 m. This implies that the subsurface contains resistive materials. The upper part of the layer reveals resistive materials at the top layer in profile 10 (Fig. 12). The resistivity values range from 4-1500 Ωm (Ohm meters) with a thickness of about 1.5 m. The northeastern part of the profile revealed very low resistivity, with resistivity values ranging between 2.4-20 Ωm at a depth range of 2-15.8 m. The high resistivity values (206-1400 Ωm) observed towards the southeastern region, at depth range of 10-15.8 m showed that the subsurface contains resistive materials. The upper part of the layer reveals resistive materials at the top layer in profile 11 (Fig. 13). The resistivity values range from 9-300 Ωm (Ohm meters) with a thickness of about 1.5 m. This layer is underlain by a basement rock which has a depth range of 1.5-7.9 m with resistivity values ranging between 15-300 Ωm.

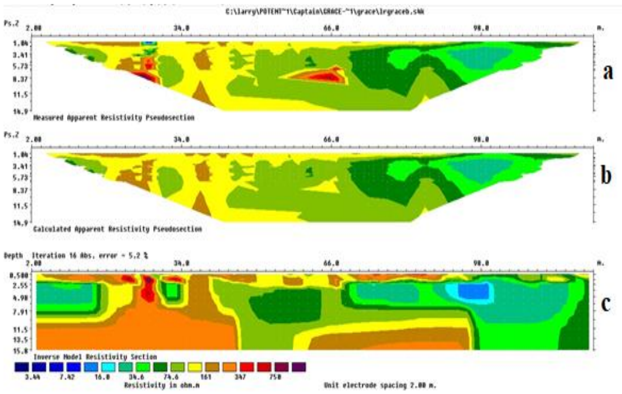

Figure 11: 2D inversion result of profile 9. (a) measured apparent resistivity pseudo-section, (b) calculated apparent resistivity pseudo-section, and (c) inverse model resistivity section.

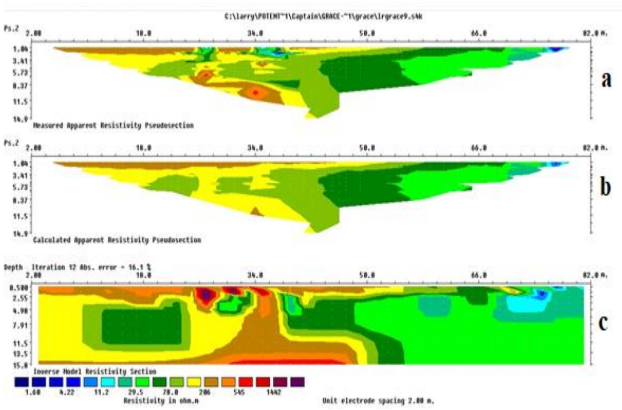

Figure 12: 2D inversion result of profile 10. (a) measured apparent resistivity pseudo-section, (b) calculated apparent resistivity pseudo-section, and (c) inverse model resistivity section.

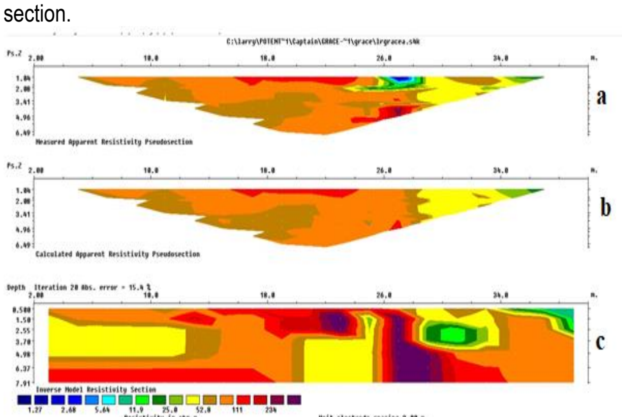

Figure 13: 2D inversion result of profile 11. (a) measured apparent resistivity pseudo-section, (b) calculated apparent resistivity pseudo-section, and (c) inverse model resistivity section.

Conclusion

The use of 2D electrical resistivity imaging survey reduces the uncertainty of locating probable region with good groundwater potential. The inverted subsurface resistivity image revealed heterogeneous lithologic units whose resistivity values range from 1 Ωm to 3500 Ωm. The study area is identified to have three geoelectric layers with varying resistivities and thickness; the top layer (topsoil) ranging from 5 Ωm to 3500 Ωm and 1.5 m to 2.55 m, the second layer (weathered/fractured basement) ranging from 1 Ωm to 3000 Ωm and 1.5 m to 15.8 m, while the third layer (bedrock) ranging from 1000 Ωm to 3500 Ωm and 10 m to 15.8 m. The weathered/fractured layer which has the lowest resistivity as compared to other layers, serves as the aquiferous layer.

REFERENCES

Adelana, S. M., & Olasehinde , P. I. (2003). High nitrate in water supply in Nigeria: Implications for human health. *Water Resources - Journal of Nigerian Association of Hydrogeologists (NAH), 14*, 1-11.

AIIC. (2009 - 2010). Abuja investor guide . *A publication of the Abuja infrastructure investment centre (AIIC)*, 176.

CIWAT. (2010). *Water supply master plan of Abuja, Nigeria.* Abuja Nigeria: Unpub. Technical Report by CIWAT Nigeria, Limited, submitted to FCT Water Board Abuja Nigeria.

Dahlin, T. (2001). The Development of DC Resistivity Imaging Techniques. *Computers and Geosciences, 27*, 1019 - 1029.

FCT MDGs. (2010). *Baseline Survey of the Federal Capital Territory, Abuja, Nigeria.* Unpublished Report for FCT MDGs office, Abuja.

Griffiths, D. H., & Barker, R. D. (1993). Two-Dimensional Resistivity Imaging and Modeling in Areas of Complex Geology. *Journal of Applied Geophysics, 29*, 211 - 266. Eweghachitere site na https://doi.org/10.1016/0926-9851(93)90005-J

Hamzah, U., Samsudin, A. R., & Ayub, S. M. (2006). Electrical Imaging of groundwater aquifer at Banting, Selangor, Malaysia. *Environ Geol, 49*, 1156 - 1162. doi:10.1007/s00254-005-0160-6

Loke, M. H., & Barker, R. D. (1996). Rapid Least-Squares Inversion of Apparent Resistivity Pseudosections by Quasi-Newton Method. *Geophysical Prospecting, 44*, 131-152. doi:10.1111/j.1365-2478.1996.tb00142.x.

Meliva, R. G. (2016). *Aquifer Characterization and Properties. In: Aquifer Characterization Techniques. Springer Hydrogeology.* Springer, Cham. https://doi.org/10.1007/978-3-319-32137-0_1

Samsudin, A. R., Hamzah, U., Rafek, A. G., & Yaacub, R. (2000). Application of Geoelectrical Resistivity Imaging for Site Investigation. *Geological Society of Malaysia Annual Geological Conference* (ibe 375-380). Pulau Pinang, Malaysia.

Samsudin, A. R., Hamzah, U., & Ramli, Z. (2001). Geophysical Investigation of the Olak Lempit Quaternary Basin, Selangor, Malaysia. *Geosea Regional Congress* (ibe 280-282), Yogyakarta, Indonesia.

Seiler, K. (2000). Man's impact on groundwater systems. In: W. G. Mook (Ed.), Environmental Isotopes in the Hydrological Cycle: Principles and applications, 5 (39), 109), *technical document in hydrology*, UNESCO-IHP.